Journal of Engineering Science and Technology
Vol. 9, No. 4 (2014) 502 - 512

OPTIMIZATION OF ELECTRICAL DISCHARGE MACHINING PARAMETERS OF ALUMINIUM HYBRID COMPOSITES USING TAGUCHI METHOD

N. RADHIKA*, A. R. SUDHAMSHU, G. KISHORE CHANDRAN

Department of Mechanical Engineering, Amrita School of Engineering
Amrita Vishwa Vidyapeetham, Coimbatore, India
*Corresponding Author: n_radhika1@cb.amrita.edu

Abstract

Metal matrix composites utilises the combined properties of the constituent material that finds applications in various fields. The present study investigates the influence of peak current, flushing pressure and pulse-on time on Electrical Discharge Machining of AlSi10Mg alloy reinforced with 3 wt% graphite and 9 wt% alumina hybrid metal matrix composites. Taguchi's Design of Experiment was used to analyse the machining characteristics of hybrid composites. Analysis of Variance and Signal-to-Noise ratio were used to determine the influence of input process parameters on the surface roughness, material removal rate and tool wear rate. Signal to Noise ratio and Analysis of Variance revealed that peak current was the most influential parameter on surface roughness followed by pulse on time and flushing pressure. For material removal rate, the major parameter was flushing pressure followed by peak current and pulse on time. The most significant parameter of tool wear rate was pulse on time followed by peak current and flushing pressure. Interaction terms also have significant effect on their output responses.

Keywords: Metal matrix composites, Electrical discharge machining, Design of experiment, Surface roughness, Material removal rate, Tool wear rate.

1. Introduction

Aluminium alloys are preferred due to its high strength to weight ratio, abundance in nature and corrosion resistance properties. But their uses are limited due to low wear resistance. In order to improve its physical properties, metal matrix composites (MMCs) are widely used. MMCs consist of at least two materials with one being metal, the other can be of different material that acts as reinforcement. Apart from

Nomenclatures

I	Peak current, A
MRR	Material removal rate, g/hr
n	Number of observations
p	Flushing pressure, kg/cm^2
Ra	Surface roughness, µm
S/N	Signal to noise ratio, dB
T_{on}	Pulse on time, µs
TWR	Tool wear rate, g/hr
y	Observed data

Abbreviations

AMMCs	Aluminium metal matrix composites
DOE	Design of experiment
EDM	Electrical Discharge Machining
MMCs	Metal matrix composites

structural support, reinforcements are also used to improve the properties of MMCs. MMCs with at least three constituents are called as hybrid composites. Combined with high specific strength and good corrosion resistance, Aluminium metal matrix composites (AMMCs) are attractive for a range of engineering applications [1]. AMMCs are used to manufacture lightweight parts due to their low density and high specific mechanical properties. In AMMCs, a hard and brittle component, which is usually ceramic is dispersed into the matrix to obtain properties that are superior to conventional alloys [2]. AMMCs are used in high tech structural and functional applications such as defence, sports, and thermal management areas, automotive and aerospace [3].

Increasing the productivity and quality of machined parts are the main challenges of metal-based industry, leading to increased interest in monitoring all aspects of the machining process .The presence of reinforcements in the matrix makes machining process difficult, due to its hard and abrasive nature. The hard reinforcement wraps around the tool-bit that leads to tool breakage [4], which in turn increases tool cost. Also, it is difficult to achieve a good surface finish in conventional machining. But wear of alumina reinforced AMMCs are less compared to other MMCs due to stable oxide layer formed by alumina [5]. With respect to high tool wear and tooling cost in conventional machining, unconventional processes offers attractive alternative [6]. Electrical Discharge Machining (EDM) is a feasible option for the experiment. In EDM, electrical discharge is used to remove material from the work piece [7, 8]. In this, the electrode or the tool acts as cathode and the work piece acts as an anode. Since there is no contact between the tool and the workpiece, no physical pressure is applied on the workpiece. A dielectric fluid acts as a medium for spark, and is also used to flush the removed material from the workpiece.

The aim of this paper is to fill the gap in the literature of the optimized machining condition such as peak current, pulse on time and flushing pressure of alumina/graphite reinforced AMMCs material to obtain minimum surface roughness, *Ra*, tool wear rate, *TWR* and maximum material removal rate, *MRR*.

2. Design of Experiment

In the competitive market, industries face challenges in bringing high quality products. Taguchi method is one of the most efficient tools which can be used to reduce the number of variations in parameters through robust design of experiments (DOE). The independent variables (parameters) used in the study are peak current, flushing pressure and pulse on time (T_{on}). Other minor parameters that affect the EDM performance include pulse off time, spark gap, voltage, current density and polarity, but the main parameters are input current, pulse on time and flushing pressure as these parameters cause the maximum deviation in the output. This has been found out by conducting the trial runs. T_{on} is the duration for which electric discharge occurs. p is the pressure of the dielectric fluid flushed on the workpiece. Their influence on *MRR*, *Ra*, and *TWR* are studied, which are the output parameters.

MRR defines the time required for machining the workpiece. Since the shape of the workpiece depends on the shape of the tool, *TWR* should be minimum in order to attain dimensional accuracy of the workpiece. The parameters and its three levels are shown in Table 1. The range is selected by taking into consideration the capacity of the machine on which the experiment is being conducted on. It is also ensured that a wide range is chosen so that optimization is more accurate. In this study, L_{27} orthogonal array is chosen wherein there are 27 rows and 9 columns.

Table 1. Parameters and Their Level.

Level	I (A)	p (kg/cm^2)	T_{on} (µs)
1	10	1.0	120
2	20	1.5	190
3	30	2.0	420

Three different values are selected for each parameter, leading to an overall combination of 27 distinct experiments. The relation between the parameters and various other relations are found out using MINITAB16 which is specifically used for DOE application. The experimental data such as *MRR*, *TWR* and *Ra* are converted to Signal-to-Noise (*S/N*) ratio. *S/N* ratio is defined as the ratio of the mean of the signal to the standard deviation of noise. It is used to determine the rank of input process parameters. There are three types of quality characteristics, namely larger the better, smaller the better and nominal the best [9]. For *Ra* and *TWR*, smaller the better characteristic is used, shown in Eq. (1), since better surface finish and longer tool life is required. For *MRR*, larger the better characteristic is used, shown in Eq. (2).

Smaller the better characteristics -

$$\frac{s}{N} = -\log 10\left[\frac{1}{n}\left(\sum y^2\right)\right] \quad (1)$$

where y is the required data (*Ra* or *TWR*) and n is the number of observations.

Larger the better characteristics –

$$\frac{s}{N} = -\log 10\left[\frac{1}{n}\left(\sum 1/y^2\right)\right] \quad (2)$$

where y is the required data (*MRR*) and n is the total number of observation [10].

With these relations, maximum *MRR* and minimum *TWR* and Ra, are found with the available process parameter. The relative effect of one parameter over the other was found using Analysis of Variance (ANOVA). It is a statistical hypothesis testing used in the analysis of experimental data. It compares the mean square of the result with deviation from sample mean. The optimized result should give minimum *Ra*, maximum *MRR*, and minimum *TWR*.

3. Experimental Setup

In this study, Electronica ZNC small die sinker machine (500×300 mm), Fig. 1, is used to drill holes of 8 mm diameter in the specimen. The specimen is cylindrical in shape with length and diameter being 22 mm and 12 mm respectively. An AC power supply of 415 V is used, with kerosene as the dielectric fluid due to its low chemical reactivity. The copper electrode and specimen are submerged in the dielectric fluid and the EDM machine is connected to the power supply.

Fig. 1. Electronica-Small Die Sinking Electric Discharge Machine.

In the control panel, based on the depth provided by the operator, the machine decides the extent of machining, i.e., the tool is moved according to the parameter set in the control panel, cutting away the material for that particular depth and leaves the finished workpiece. The power supply generates an electrical potential between the electrode and work piece. Due to high potential generated, sparks are generated between the two nearest points of the two electrodes. The sparks in this region melts or vaporizes the specimen at the contact point. To avoid excessive heat, the current is passed intermittently for a particular duration known as pulse on time (T_{on}).The burnt material settles around the surface of tool and specimen.

The dielectric fluid flushes away the burnt material (also referred to as debris) and dissipates the heat produced by sparks. Time for complete machining of the specimen is noted. This procedure is repeated for all the experiments. The work piece and electrode are weighed before and after the machining process to calculate the *MRR* and *TWR*. Stylus type *Ra* tester (TESA RUGOSURF 10G) is used to measure the *Ra* of the workpiece corresponding to each machining

condition. *MRR* and *TWR* for each experiment are calculated using the following expressions, shown in Eq. (3) and Eq. (4) respectively.

$$MRR = \frac{\text{initial mass of workpiece} - \text{final mass of workpiece}}{\text{machining time}} \quad (3)$$

$$TWR = \frac{\text{initial mass of electrode} - \text{final mass of electrode}}{\text{machining time}} \quad (4)$$

4. Results and Discussion

Detailed analysis of *S/N* ratio and ANOVA has been carried out to find the percentage effect of each input parameters on the response. All the experimental conditions and their output values are shown in Table 2.

Table 2. L_{27} Orthogonal Array and its Output Parameters.

S. No.	*I*	*p*	T_{on}	Ra	S/N for Ra	MRR	S/N for MRR	TWR	S/N for TWR
	A	kg/cm^2	µs	µm	dB	g/hr	dB	g/hr	dB
1	10	1.0	120	3.085	-9.7851	19.088	25.615	0.2299	12.766
2	10	1.0	190	3.385	-10.591	17.019	24.619	0.1064	19.460
3	10	1.0	420	3.214	-10.140	21.404	26.610	0.0403	27.886
4	10	1.5	120	2.349	-7.4177	19.866	25.962	0.2004	13.961
5	10	1.5	190	3.414	-10.665	16.106	24.140	0.1051	19.561
6	10	1.5	420	2.910	-9.2779	17.011	24.615	0.0267	31.462
7	10	2.0	120	3.132	-9.9164	16.746	24.478	0.1875	14.539
8	10	2.0	190	2.372	-7.5023	10.435	20.370	0.0602	24.396
9	10	2.0	420	2.632	-8.4057	13.561	22.646	0.4096	7.751
10	20	1.0	120	3.014	-9.5829	27.180	28.685	0.4268	7.395
11	20	1.0	190	3.639	-11.219	23.374	27.374	0.2997	10.464
12	20	1.0	420	3.376	-10.568	25.234	28.039	0.0976	20.205
13	20	1.5	120	2.823	-9.0142	19.023	25.585	0.3613	8.841
14	20	1.5	190	3.653	-11.253	17.032	24.625	0.2565	11.817
15	20	1.5	420	4.063	-12.176	22.666	27.107	0.1178	18.574
16	20	2.0	120	3.362	-10.532	14.593	23.283	0.2676	11.447
17	20	2.0	190	2.712	-8.6658	16.032	24.100	0.2126	13.445
18	20	2.0	420	5.609	-14.977	20.307	26.153	0.0948	20.455
19	30	1.0	120	3.776	-11.540	23.912	27.572	0.3874	8.236
20	30	1.0	190	5.509	-14.821	24.927	27.933	0.3774	8.462
21	30	1.0	420	5.570	-14.917	26.214	28.370	0.1439	16.838
22	30	1.5	120	5.662	-15.059	18.814	25.489	0.3481	9.163
23	30	1.5	190	6.282	-15.962	19.818	25.941	0.2667	11.478
24	30	1.5	420	6.491	-16.246	23.125	27.281	0.1603	15.896
25	30	2.0	120	4.680	-13.404	19.841	25.951	0.3554	8.985
26	30	2.0	190	6.570	-16.351	18.262	25.231	0.2251	12.949
27	30	2.0	420	6.801	-16.651	21.537	26.664	0.1508	16.426

4.1. Influence of parameters on surface roughness

The *S/N* ratio analysis has been used to determine the influence of input parameters on the output. In this analysis, rank denotes the influence of the input parameter on the output. Table 3 shows the *S/N* ratio for *Ra*. The result revealed that peak current is the most significant parameter for *Ra* followed by pulse on time and flushing pressure.

Table 3. Response Table for Signal-to-Noise Ratios – Surface Roughness.

Level	I (A)	p (kg/cm^2)	T_{on} (µs)
1	-9.300	-11.463	-10.695
2	-10.888	-11.897	-11.892
3	-14.995	-11.823	-12.596
Delta	5.695	0.434	1.901
Rank	1	3	2

From Figs. 2(a) and 2(c), it is observed that *Ra* increases with peak current and pulse on time respectively. As peak current increases, the intensity of the spark increases. Presence of alumina in the spark gap leads to increase in *Ra*. As pulse on time increases, the duration for which discharge occurs is increased. This leads to formation of molten material craters on the workpiece causing increase in *Ra* [11]. Increase in both T_{on} and peak current lead to increase in surface irregularities [12]. The *Ra* also increases with increase in flushing pressure, Fig. 2(b). As pressure increases, the velocity decreases which in turn reduces heat dissipation, leading to alumina and graphite debris on the walls, which leads to increase in *Ra*. From Fig. 2(b), the marginal decrease in *Ra* with increase in flushing pressure is due to the presence of graphite particles that act as self-lubricant [13].The optimal machining condition to obtain minimum *Ra* is found to be I = 10 A, p = 1.0 kg/cm^2, T_{on}=120 µs.

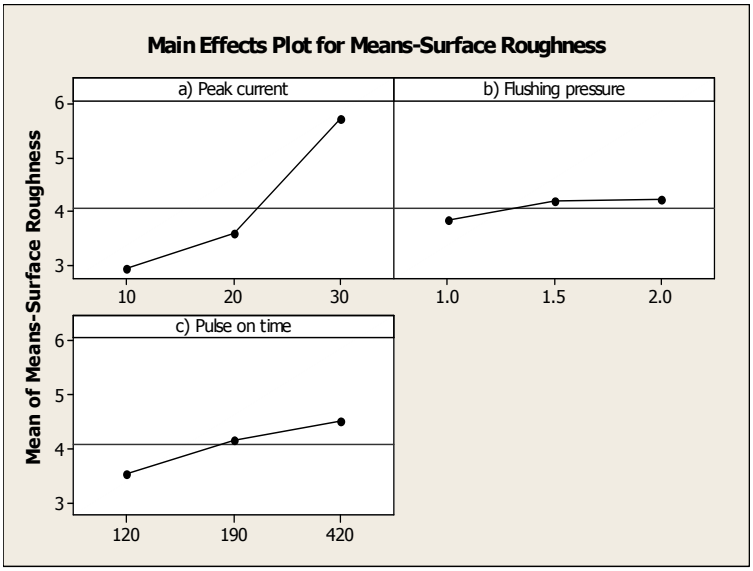

Fig. 2. Main Effects Plot for Surface Roughness.

4.2. Influence of parameters on material removal rate

Table 4 shows the response table for *MRR*. It is observed from the response table that, flushing pressure is the most influential parameter for *MRR* followed by peak current and pulse on time.

Table 4. Response Table for Signal-to Noise Ratios – Material Removal Rate.

Level	I (A)	p (kg/cm^2)	T_{on} (µs)
1	24.34	27.20	25.85
2	26.11	25.64	24.93
3	26.72	24.32	26.39
Delta	2.38	2.88	1.46
Rank	2	1	3

Figure 3 shows the main effect plots for *MRR*. It is observed from the graph Fig. 3(a) that *MRR* increases with increase in peak current. As peak current increases, kinetic energy of the spark increases, leading to increase in temperature. Hence, melting and vaporization of material increases which leads to increase in *MRR* [14]. The *MRR* decreases and then increases after a certain threshold point with increase in T_{on}, Fig. 3(c). The alumina particle which is dispersed from the metal matrix obstructs the spark gap and gets heated by the discharge which reduces *MRR*. After acquiring high thermal energy, alumina gets vaporised which leads to increase in *MRR*. The decrease in *MRR* is due to arcing that leads to decrease in discharge energy and high heat produced [15]. Further increment in T_{on} leads to vaporisation of alumina leading to rise in *MRR*. The *MRR* decreases with increase in flushing pressure, Fig. 3(b). As flushing pressure increases, the inlet velocity decreases and the rate of removal of debris is reduced. This increases the concentration of debris in the gap and hinders *MRR*. Addition of graphite helps in the removal of debris from the spark gap that leads to increase in *MRR* [16]. The optimal machining condition to obtain maximum *MRR* was found to be I = 30 A, p = 1.0 kg/cm^2, T_{on} = 420 µs.

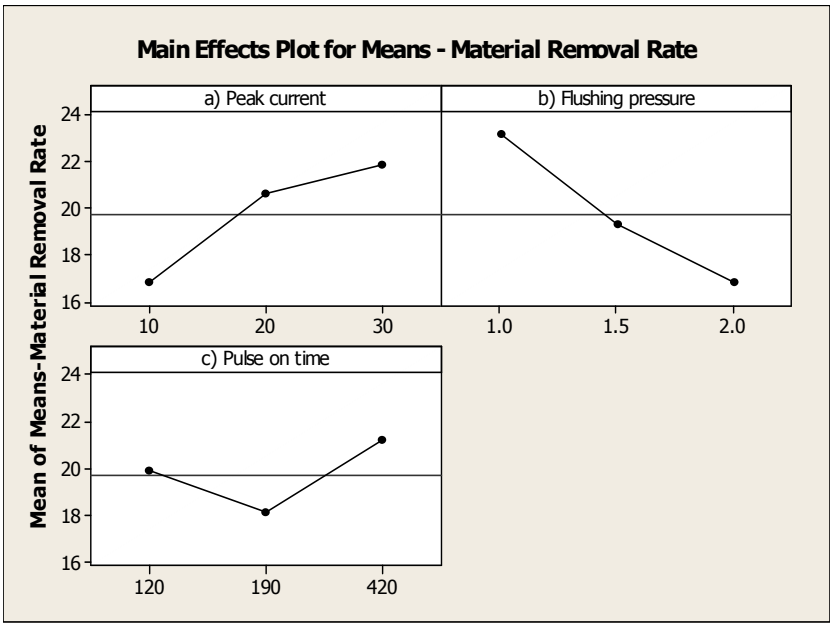

Fig. 3. Main Effects Plot for Means- Material Removal Rate.

4.3. Influence of parameters on tool wear rate

Table 5 shows the order of ranking of input parameters for *TWR*. The result revealed that T_{on} is the most significant parameter for *TWR* followed by peak current and flushing pressure.

Table 5. Response Table for Signal-to Noise Ratios – Tool Wear Rate.

Level	*I* (A)	*p* (kg/cm^2)	T_{on} (µs)
1	19.09	14.64	10.59
2	13.63	15.64	14.67
3	12.05	14.49	19.50
Delta	7.04	1.15	8.91
Rank	2	3	1

Figure 4 shows the main effect plot for *TWR*. It is observed from Fig. 4(a) that as peak current increases, the *TWR* increases and is due to the abrasive nature of the hard reinforcement, alumina [17]. Figure 4(b) shows as flushing pressure decreases, the inlet velocity increases which reduces the concentration of debris in the tool surface and reduces wear. After a certain point, the decrease in velocity leads to increase in concentration of debris and hence blocking the contact between the electrode leading to rise in temperature causes tool wear [18]. As T_{on} increases, Fig. 4(c), the tool wear decreases due to the deposit of decomposed graphite on the tool surface [19]. The optimal machining condition to obtain minimum *TWR* is found to be $I = 10$ A, $p = 1.5$ kg/cm^2, $T_{on} = 420$ µs.

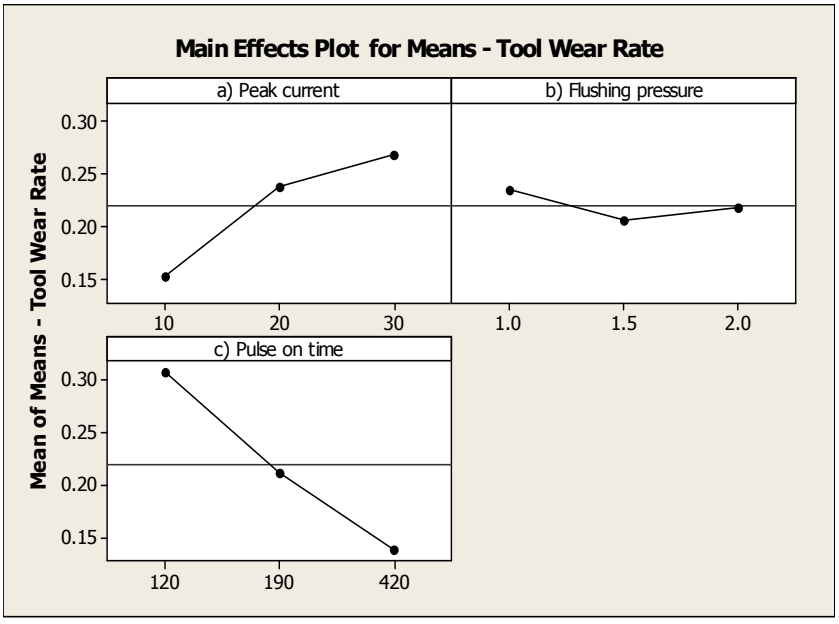

Fig. 4. Main Effect Plot for Tool Wear Rate.

4.4. Analysis of variance and significance of parameters

ANOVA is used to determine the influence of input parameters on the response quantitatively. Tables 6, 7 and 8 show the results of ANOVA for *Ra*, *MRR* and *TWR* respectively. Confidence level of 95% is utilised for the analysis.

Table 6. Analysis of Variance for Surface Roughness.

Source of Variation	DF	Seq SS	Adj SS	Adj MS	*F*-test	*P*-value	*P*%
I	2	90.650	90.650	45.325	51.50	0.000	69.18
p	2	7.970	7.970	3.9853	4.53	0.048	6.08
T_{on}	2	15.167	15.167	7.5837	8.62	0.010	11.57
$I \times p$	4	5.7980	5.7980	1.4495	1.65	0.254	4.42
$I \times T_{on}$	4	2.3910	2.3910	0.5977	0.68	0.625	1.82
$p \times T_{on}$	4	2.0126	2.0126	0.5032	0.57	0.691	1.53
Error	8	7.0403	7.0403	0.8800			5.37
Total	26	131.030					100

Notes: DF, Degrees of freedom; Seq SS, Sequential sum of squares; Adj SS, Adjusted sum of squares; Adj MS, Adjusted mean squares; *P*, Percentage of Contribution.

Table 7. Analysis of Variance for Material Removal Rate.

Source of Variation	DF	Seq SS	Adj SS	Adj MS	*F*-test	*P*-value	*P*%
I	2	123.530	123.530	61.765	15.64	0.002	29.08
p	2	183.747	183.747	91.873	23.27	0.000	43.26
T_{on}	2	44.026	44.026	22.013	5.57	0.030	10.36
$I \times p$	4	20.710	20.710	5.177	1.31	0.344	4.87
$I \times T_{on}$	4	19.934	19.934	4.984	1.26	0.360	4.69
$p \times T_{on}$	4	1.128	1.128	0.2823	0.07	0.989	0.26
Error	8	31.592	31.592				7.43
Total	26	424.667					100

Table 8. Analysis of Variance for Tool Wear Rate.

Source of Variation	DF	Seq SS	Adj SS	Adj MS	*F*-test	*P*-value	*P*%
I	2	0.065660	0.065660	0.032780	6.25	0.023	17.41
p	2	0.003953	0.003953	0.001976	0.38	0.698	1.05
T_{on}	2	0.129423	0.129423	0.064711	12.33	0.004	34.38
$I \times p$	4	0.033072	0.033072	0.008268	1.58	0.270	8.78
$I \times T_{on}$	4	0.054460	0.054460	0.013615	2.59	0.117	14.47
$p \times T_{on}$	4	0.048041	0.048041	0.012010	2.29	0.148	12.76
Error	8	0.041977	0.041977	0.005274			11.15
Total	26	0.376486					100

It is observed from Table 6 that peak current has the highest influence (69.18%) on *Ra* followed by pulse on time (11.57%) and flushing pressure (6.08%). Among interaction terms, interaction between *I* and *p* has 4.42%, interaction between *I* and T_{on} has 1.82% and interaction between *p* and T_{on} has 1.53%. This indicates that interaction terms also had significant effect on *Ra*. Table 7 reveals that flushing pressure has maximum influence (43.26%) on *MRR* followed by peak current (29.08%) and pulse on time (10.36%). Interaction

parameters also have significant effect on the output response. From Table 8, it is observed that pulse on time has the highest statistical influence (34.38%) on *TWR* wear rate followed by peak current (17.41) and flushing pressure (1.05). Interaction between $I \times p$ has an influence of 8.78%, interaction between $I \times T_{on}$ has an influence of 14.47% and interaction between $p \times T_{on}$ has an influence of 12.76% on *TWR* of aluminium composites.

5. Conclusions

Signal-to-Noise ratio analysis shows that the peak current is the most dominant factor in influencing surface roughness. For material removal rate, dominant factor is flushing pressure, whereas for tool wear rate it is found to be pulse on time. The Taguchi method analysis of experimental results gave the optimal setting of control parameters which would result in minimum surface roughness and tool wear rate, and maximum material removal rate. The percentage effect of input parameters on surface roughness, material removal rate and tool wear rate, and its interactions are found with Analysis of Variance results. Surface roughness increase is mainly attributed to increase in peak current due to non-uniform material removal. Surface roughness also increases due to rise in flushing pressure due to accumulation of alumina. Material removal rate is inversely proportional to flushing pressure as reduced flow velocity of dielectric reduces debris removal rate. Tool wear rate reduces with increase in pulse on time due to deposition of graphite.

References

1. Hashim, J.; Looney, L.; and Hashmi, M.S.J. (1999). Metal matrix composites: Production by stir casting method. *Journal of Materials Processing Technology*, 92-93, 1-7.
2. Srivatsan, T.S.; Ibrahim, I.A.; Mohamed, F.A.; and Lavernia, E.J. (1991). Processing techniques for particulate reinforced metal aluminium matrix composites. *Journal of Material Science*, 26(22), 5965-5978.
3. Surappa, M.K. (2003). Aluminium matrix composites: Challenges and opportunities. *Sadhana*, 28(1-2), 319-334.
4. Mouangue, N.A.; Abdul-Rani, A.M.; Ahmad, F.; Zainuddin, A.; and Jason, L.S.H. (2011). Effects of electro-discharge machining on aluminium metal matrix composite. *Journal of Applied Science*, 11(9), 1668-1672.
5. Radhika, N.; Subramanian, R.; and Venkat, P.S. (2011). Tribological behaviour of aluminium/alumina/graphite hybrid metal matrix composite using Taguchi's techniques. *Journal of Minerals and Material Characterization and Engineering*, 10(5), 427-443.
6. Saini, V.K.; Zahid, A.K.; and Siddiquee, A.N. (2012). Advancements in non-conventional machining of aluminium metal matrix composite materials. *International Journal of Engineering Research and Technology*, 1(3), 1-14.
7. Tomadi, S.H.; Hassan, M.A.; Hamedon, Z.; Daud, R.; and Khalid, A.G. (2004). Analysis of the influence of EDM parameters on surface quality, material removal rate and electrode wear of tungsten carbide. *Proceeding of the International Multi Conference of Engineers and Computer Scientists*, Hong Kong, 1803-1808.

8. Gao, Q.; Zhang, Q.-H.; Su, S.-P.; and Zhang, J.-H. (2008). Parameter optimization model in electrical discharge machining process. *Journal of Zhejiang University SCIENCE A*, 9(1), 104-108.
9. Puri, Y.M.; and Deshpande, N.V. (2004). Simultaneous optimization of multiple quality characteristics of wedm based on fuzzy logic and Taguchi technique. *Proceedings of the Fifth Asia Pacific Industrial Engineering and Management Systems Conference*, Gold Coast, Australia, 14.18.1- 14.18.12.
10. Sharma, N.K.; and Cudney, E.A. (2011). Signal-to-noise ratio and design complexity based on unified loss function - LTB case with finite target. *International Journal of Engineering Science and Technology*, 3(7), 15-24.
11. Shabgard, M.; Seyedzavvar, M.; and Oliaei, S.N.B. (2011). Influence of input parameters on the characteristics of the EDM process. *Journal of Mechanical Engineering*, 57(9), 689-696.
12. Ben Salem, S.; Tebni, W.; and Bayraktar, E. (2011). Prediction of surface roughness by experimental design methodology in electrical discharge machining (EDM). *Journal of Achievements in Material and Manufacturing Engineering*, 49(2), 150-157.
13. Yan, B.H.; and Wang, C.C. (1999). The machining characteristics of Al_2O_3/6061Al composite using rotary electro-discharge machining with a tube electrode. *Journal of Material Processing Technology*, 95(1-3), 222-231.
14. Kathiresan, M.; and Sornakumar, T. (2010). EDM studies on aluminum alloy-Silicon carbide composites developed by vortex technique and pressure die casting. *Journal of Minerals and Material Characterization and Engineering*, 9(1), 79-88.
15. Shamsul, S.M.Y. (2008). *Effects of flushing on electro-discharge machined surface*. Dissertation Thesis, Universiti Malaysia Pahang, Kuantan and Pekan, Pahang, Malaysia, 11-12.
16. Ozgedik, A.; and Cogun, C. (2006). An experimental investigation of tool wear in electric discharge machining. *The International Journal of Advanced Manufacturing Technology*, 27(5-6), 488-500.
17. Hayajneh, M.T.; Hassan, A.M.; and Al-Omari, M.A. (2001). The effect of graphite particles addition on the surface finish of machined Al-4 Wt.% Mg alloys. *Journal of Material Engineering and Performance*, 10(5), 521-525.
18. Suhail, A.H.; Ismail, N.; Wong, S.V.; and Abdul Jalil, N.A. (2010). Optimization of cutting parameters based on surface roughness and assistance of workpiece surface temperature in turning process. *American Journal of Engineering and Applied Science*, 3(1), 102-108.
19. Venkat, P.S.; Subramanian, R.; Praveen, N.; and Arun, L. (2011). Electric discharge machining of AlSi10Mg/Fly ash/graphite hybrid metal matrix composites. *European Journal of Scientific Research*, 59(4), 485-498.